Clinical significance of visually equivocal amyloid PET findings from the Alzheimer's Disease Neuroimaging Initiative cohort

Minyoung Oh[a], Minjung Seo[c], Sun Young Oh[b], Heeyoung Kim[d], Byung Wook Choi[e], Jungsu S. Oh[a] and Jae Seung Kim[a]; For the Alzheimer's Disease Neuroimaging Initiative

To evaluate the clinical and imaging characteristics of patients with visually equivocal amyloid PET images, patients from the Alzheimer's Disease Neuroimaging Initiative cohort who had fluorine-18-florbetapir PET scans both at baseline and 24 months were selected. Five nuclear medicine physicians visually assessed the PET images and classified them as either positive or negative. Images not reaching a majority agreement were classified as equivocal. Among a total of 379 patients, the number of patients in each fluorine-18-florbetapir PET negative/equivocal/positive categories was 218 (57.5%), 32 (8.4%), and 129 (34.0%). Eight to 9% of patients with normal cognition ($N = 12/141$), mild cognitive impairment ($N = 20/214$), and no Alzheimer's disease ($N = 0/24$) showed equivocal PET finding for each. In negative/equivocal/positive groups, positive cerebrospinal fluid $A\beta_{1-42}$ was observed in 25.7, 81.5, and 98.3%, respectively. Baseline standardized uptake value ratios of fluorine-18-florbetapir PET were 0.75 ± 0.05, 0.86 ± 0.09, and 1.01 ± 0.09, respectively [$F_{(2, 376)} = 603.547$; $P < 0.001$]. After 24 months of follow-up, the standardized uptake value ratios increased by 0.81 ± 2.62, 2.81 ± 2.90, and $2.17 \pm 3.66\%$, respectively [$F_{(2, 376)} = 7.905$, $P < 0.05$ vs. the negative group]. Among mild cognitive impairment patients, the equivocal group showed a more rapid decline in glucose metabolism than the negative group [5.52 ± 5.36 vs. 0.67 ± 4.45; $F_{(2, 122)} = 9.028$, $P < 0.01$]. 8.4% of the patients in this study showed a visually equivocal result of amyloid PET. These patients showed a moderate amount of amyloid accumulation and a rapid rate of accumulation. *NeuroReport* 29:553–558 Copyright © 2018 Wolters Kluwer Health, Inc. All rights reserved.

[a]Department of Nuclear Medicine, Asan Medical Center, University of Ulsan College of Medicine, [b]Department of Nuclear Medicine, National Police Hospital, Seoul, [c]Department of Nuclear Medicine, Ulsan University Hospital, University of Ulsan College of Medicine, Ulsan, [d]Department of Nuclear Medicine, Kosin University Gospel Hospital, Kosin University College of Medicine, Busan and [e]Department of Nuclear Medicine, Daegu Catholic University Medical Center, School of Medicine, Catholic University of Daegu, Daegu, Korea

Correspondence to Jae Seung Kim, MD, PhD, Department of Nuclear Medicine, Asan Medical Center, University of Ulsan College of Medicine, 88, Olympic-ro 43-gil, Songpa-gu, Seoul 05505, Korea
Tel: + 82 230 104 594; fax: + 82 230 104 588; e-mail: jaeskim@amc.seoul.kr

Received 10 November 2017 accepted 17 January 2018

Introduction

Alzheimer's disease (AD) accounts for 60–70% of all dementia and is characterized by irreversible memory impairment, behavioral disturbances, and β-amyloid deposition in the cerebral cortex [1]. To identify brain β-amyloid accumulation, C-11 Pittsburgh compound B PET imaging was used widely [2], and fluorine-18-labeled amyloid PET tracers have been approved for the same purpose in USA and Europe [3]. Regulatory approval states that fluorine-18 amyloid PET images should be classified in a binary (positive/negative) manner by visual read. On the positive PET images, the specific accumulation of β-amyloid in gray matter causes it to have higher signal intensity than white matter. In contrast, only nonspecific accumulation in white matter is observed on the negative PET images. Visual assessment of amyloid PET images, however, can result in equivocal ratings [4–7]. They could be because of high interobserver variability or variable β-amyloid kinetics or a third category with intermediate amyloid load. Assessment of clinical characteristics and long-term change in the cognitive function of patients with equivocal PET images is necessary because pathologic confirmation of PET findings is difficult at diagnosis.

In this study, we evaluated the clinical and imaging characteristics and longitudinal change of patients with visually equivocal amyloid PET images from the Alzheimer's Disease Neuroimaging Initiative (ADNI) [8] to determine the clinical significance of equivocal amyloid PET images.

Patients and methods
Participants

We included patients with cognitively normal (NC) or subjective memory impairment (SMI), mild cognitive impairment (MCI), and AD who had fluorine-18-florbetapir PET scans at baseline and at 24-month follow-up

(F/U) as of June 2015 as a part of the ADNI study. All ADNI data are publicly available at *http://www.loni.ucla.edu/ADNI*. The ADNI study was approved by the Institutional Review Board of the respective institutions before beginning the study. Informed consent was obtained from all participants.

Fluorine-18-florbetapir PET image processing and analysis

Fluorine-18-florbetapir PET images were acquired 50–70 min after injection; these images were then realigned, averaged, and resliced to a common voxel size (1.5 mm^3), which were later smoothed to a common resolution of 8-mm full-width at half-maximum (FWHM).

Baseline structural MRI were co-registered with fluorine-18-florbetapir PET images from each participant; these images were then used to extract weighted cortical retention mean uptake from frontal, parietal, cingulate, and temporal regions. Standardized uptake value ratios (SUVRs) were calculated using a composite region made up of the whole cerebellum, pons, and eroded subcortical white matter as the reference region [9] with a positivity threshold of 0.79 as described previously [10,11]. Compared with the cerebellum and pons alone, reference regions that included subcortical white matter resulted in change measurements that are more accurate [9,12].

For the best visual analysis, we performed harmonization of different PET scanners. Because the uniform 8-mm FWHM resolution provided by ADNI data was mainly designed for accommodating PET images from all scanners into the same spatial resolution, the final PET images were severely degraded to the level of the scanner with the poorest spatial resolution. To avoid excessive blurring effect, we decided to harmonized the spatial resolution as that of the routine amyloid imaging protocol at our institution (Asan Medical Center). We used a post-Gaussian smoothing kernel size of 4-mm FWHM. Accordingly, postsmoothing kernel sizes of other scanners were adjusted using the following equation and the harmonization kernel information reported by Joshi *et al.* [13].

$$FWHM_{final} = \sqrt{FWHM_{Joshi}^2 + FWHM_{AMC}^2 - 8^2}.$$

A panel of five independent board-certified nuclear medicine physicians assessed all fluorine-18-florbetapir PET images; they were blinded to all clinical and diagnostic information. A binary scale was used to classify each scan – 0 if there was no significant fluorine-18-florbetapir cortical retention or 1 if there was some significant fluorine-18-florbetapir cortical retention as described previously [14]. All observers received electronic fluorine-18-florbetapir PET clinical training (*http://www.amyvidtraining.com*; Avid Radiopharmaceuticals, Philadelphia, Pennsylvania, USA), followed by assessment of 100 practice cases before actual visual assessment. The visual analysis results of fluorine-18-florbetapir PET images were classified into three categories. (a) Positive scan: if more than four observers rated as 1, (b) negative scan: if more than four observers rated as 0, and (c) equivocal scan: if there were no more than four observers with the same ratings.

Fluorine-18-fluorodeoxyglucose PET image processing

Each fluorine-18-fluorodeoxyglucose PET image was spatially normalized to the standard O-15 H$_2$O PET template using SPM5 and the extracted mean fluorine-18-fluorodeoxyglucose uptake for each participant from a set of study-independent and previously validated regions of interest (metaROIs) located in the right and left inferior temporal and lateral parietal regions, and a bilateral posterior cingulate cortex region relative to the mean of a pons and cerebellar vermis reference region [15].

Cerebrospinal fluid analysis

Cerebrospinal fluid (CSF) Aβ_{1-42}, t-tau, and p-tau were measured concurrently by fluorine-18-florbetapir scans at baseline and analyzed at the ADNI Biomarker core laboratory. We applied autopsy-validated CSF Aβ_{1-42}, t-tau, and p-tau positivity cut-offs of 192, 93, and 23 pg/ml, respectively, which were utilized in a previous study [16].

Structural MRI analyses

Cross-sectional structural differences were assessed using hippocampal volumes defined on MPRAGE images by Freesurfer v5.1 and divided by the total intracranial volume to adjust for head size.

Clinical and cognitive measurements

We examined several clinical and cognitive performance measurements including baseline and longitudinal performance on the Mini-Mental State Examination (MMSE) [17], the Rey Auditory Verbal Learning Test (RAVLT) [18], and the Alzheimer's Disease Assessment Scale-cognitive subscale (ADAS-cog) [19]. The average available F/U duration for longitudinal cognitive and biomarker measurements was 23.9 ± 1.9 months. We also examined the clinical profiles including the clinical diagnosis at baseline and 24-month F/U and whether conversion to AD occurred during the F/U period.

Statistical analysis

We used the χ^2-test for categorical variables and one-way analysis of variance for quantitative variables. *P* values were two-sided and considered statistically significant at less than 0.05 for global comparison and at less than 0.05/3 for subgroup analyses to take into account the multiple comparisons. Interobserver agreement of the visual assessment was calculated at the patient level using κ values. Analyses were carried out using statistical package for the social sciences software (version 18.0; SPSS Inc., Chicago, Illinois, USA).

Results

Demographic and clinical variables

Demographical data of the patients included as well as their clinical, cognitive, and biomarker characteristics at the time of the scan and 24-month F/U are presented in Table 1. Among a total of 379 patients, the numbers of fluorine-18-florbetapir negative/equivocal/positive patients were 218 (57.5%), 32 (8.4%), and 129 (34.0%), respectively. About 8–9% of patients with NC or subject memory impairment (NC or SMI, $N = 12/141$), MCI ($N = 20/214$), and no AD ($N = 0/24$) showed equivocal fluorine-18-florbetapir PET for each. Among the 32 patients in the equivocal group, 13 (40.6%) showed diffuse mild amyloid retention in the entire cerebral cortex. Among the rest of the patients, retention was the most common in the temporal cortex ($N = 7$, 21.9%), followed by the frontal cortex ($N = 6$, 18.8%), posterior cingulate gyrus ($N = 3$, 9.4%), and occipital cortex ($N = 3$, 9.4%). In visual interpretation using binary criteria, Fleiss' κ value of five raters was 0.78 ($P < 0.001$, $z = 48.2$).

Biomarkers

The majority of the patients in the negative group were apolipoprotein E4− (APOE4−) (78%), whereas the patients in the positive group showed the opposite pattern (75.2% APOE4+). The equivocal group showed an intermediate pattern (56.4% APOE4+).

Fluorine-18-florbetapir SUVR showed an increasing tendency in the negative/equivocal/positive group at baseline [0.75 ± 0.05, 0.86 ± 0.09, and 1.01 ± 0.09, respectively, $F(2, 376) = 603.547$, $P < 0.01$]. As shown in Fig. 1, the equivocal group among patients with MCI showed higher SUVR than did those in the negative group [0.88 ± 0.07 vs. 0.76 ± 0.04; $F(2, 211) = 291.242$, $P < 0.001$], and all of them were above the positivity threshold (0.79). The equivocal group in patients with NC or SMI showed a similar tendency [0.83 ± 0.10 vs. 0.75 ± 0.05; $F(2, 140) = 140.252$, $P < 0.001$], but they were distributed both over and below the threshold. The SUVR of the equivocal and the positive group increased more rapidly

Table 1 Demographics, clinical, and biomarker variables of patients with negative/equivocal/positive fluorine-18-florbetapir PET images

	Negative ($n = 218$)	Equivocal ($n = 32$)	Positive ($n = 129$)
Demographics			
Age (years)	71.0 ± 7.4	72.7 ± 7.6	73.5 ± 6.4
Sex (male/female) (n)	122/96	17/15	70/59
Education (years)	16.6 ± 2.5	16.8 ± 2.6	16.1 ± 2.7
Clinical [n (%)]			
NC + SMI	109 (50.0)[a]	12 (40.0)[a]	20 (15.5)[a]
MCI	106 (48.6)[a]	20 (60.0)[a]	88 (68.2)[a]
AD	3 (1.4)[a]		21 (16.3)[a]
Conversion to AD	5 (2.3)[a]	1 (3.1)[a]	20 (18.5)[a]
Biomarkers (baseline)			
ApoE4 + (%)	22.0[a]	56.4[a]	75.2[a]
18F-florbetapir (SUVR, composite)	0.75 ± 0.05	0.86 ± 0.09[b,d]	1.01 ± 0.09[b,c]
18F-florbetapir + (SUVR, composite) (%)	15.6[a]	78.1[a]	99.2[a]
^{18}F-FDG metaROI	1.33 ± 0.11	1.31 ± 0.11	1.29 ± 0.14
Hippocampal volume/ICV (%)	0.50 ± 0.07	0.48 ± 0.06	0.44 ± 0.08[b,c]
CSF Aβ_{1-42} (pg/ml)	215.12 ± 40.27[b]	166.84 ± 39.57[b]	133.30 ± 23.11[b]
CSF Aβ_{1-42}, +/− (n)	50/144	22/5	121/2
CSF Aβ_{1-42}, + (%)	25.7[a]	81.5[a]	98.3[a]
CSF p-tau (pg/ml)	30.06 ± 16.10	43.22 ± 18.83	59.67 ± 29.15
CSF p-tau, +/− (n/N)	120/74	25/2	116/7
CSF p-tau, + (%)	61.9[a]	92.6[a]	94.3[a]
CSF t-tau (pg/ml)	59.51 ± 28.53	81.9 ± 33.15	120.03 ± 56.34
CSF t-tau, +/− (n/N)	23/171	9/18	78/45
CSF t-tau, + (%)	11.9[a]	33.3%[a]	63.4[a]
Biomarkers (changes during 24 months)			
18F-florbetapir (composite) (24 months baseline) (%)	0.81 ± 2.62	2.81 ± 2.90[b]	2.17 ± 3.66[b,c]
^{18}F-FDG metaROI (baseline 24 months) (%)	1.24 ± 4.62	1.41 ± 10.47	4.46 ± 5.97[b]
Hippocampus/ICV (baseline 24 months) (%)	2.74 ± 4.17	2.95 ± 2.79	7.22 ± 5.56[b,c]
Cognitive function (baseline)			
MMSE (score)	28.76 ± 1.48	28.09 ± 1.87	27.00 ± 2.65[b,c]
ADAS-cog (score)	10.9 ± 5.36	13.34 ± 6.11	19.01 ± 8.99[b,c]
RAVLT fr (score)	4.07 ± 2.59	3.53 ± 2.05	5.05 ± 2.44[b,c]
Cognitive function (changes during 24 months)			
MMSE (baseline 24 months)	0.66 ± 3.59	-0.28 ± 2.33	2.20 ± 3.03[b,c]
ADAS-cog (24 months baseline)	-1.32 ± 4.39	-1.88 ± 3.94	4.16 ± 7.53[b,c]
RAVLT fr (baseline 24 months)	0.05 ± 3.23	-0.34 ± 3.48	-0.07 ± 2.73

Mean ± SD shown for continuous variables and proportion positive/abnormal shown for dichotomous variables.
ADAS-cog, Alzheimer's Disease Assessment Scale-cognitive subscale; AD, Alzheimer's disease; CSF, cerebrospinal fluid; 18F-florbetapir, fluorine-18-florbetapir; ^{18}F-FDG, fluorine-18-fluorodeoxyglucose; ICV, intracranial volume; metaROI, previously validated region of interest; MCI, mild cognitive impairment; MMSE, Mini-Mental State Examination; NC, normal cognition; RAVLT fr, Rey Auditory Verbal Learning Test free recall; SMI, surjective memory impairment; SUVRs, standardized uptake value ratios.
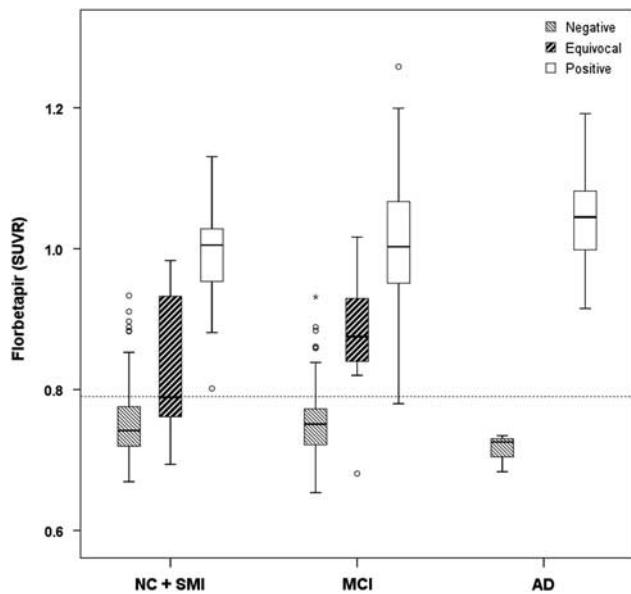[a]$P < 0.05$, for comparison among three groups.
[b]$P < 0.01$, compared with the negative group.
[c]$P < 0.01$, compared with the equivocal group.
[d]$P < 0.01$, compared with the positive group.

Fig. 1

Fluorine-18-florbetapir standardized uptake value ratios in the negative/equivocal/positive group according to clinical disease status.
AD, Alzheimer's disease; MCI, mild cognitive impairment; NC, normal cognition; SMI, surjective memory impairment; SUVRs, standardized uptake value ratios.

than that of the negative group $[2.81 \pm 2.90, 2.17 \pm 3.66$ vs. $0.81 \pm 2.62; F(2, 376) = 7.905, P = 0.004]$ during 24-month F/U.

Decreasing tendency was observed in CSF $A\beta_{1-42}$ and increasing tendency was observed in CSF p-tau and t-tau in the three groups. The majority of the patients in the equivocal (77.8%) and positive (98.3%) group were positive in both CSF $A\beta_{1-42}$ and SUVR. At baseline, the three groups did not differ significantly in hypometabolism in characteristic AD (metaROI) regions, but the positive group showed a more rapid decline (Table 1). Among the patients with MCI, the equivocal group showed a more rapid decline in glucose metabolism than those in the negative group $[5.52 \pm 5.36$ vs. $0.67 \pm 4.45; F(2, 122) = 9.028, P < 0.01]$. The positive group showed significant hippocampal atrophy at baseline $[F(2, 331) = 26.448, P < 0.01]$ and rapid progression $[F(2, 264) = 22.580, P < 0.01]$ than the other groups (Table 1).

Cognitive function
The positive group showed significantly poor performance than the other groups on MMSE, ADAS-cog, and RAVLT at baseline $[F(2, 374) = 31.513, P < 0.01]$ as well as rapid progression $[F(2, 371) = 32.336, P < 0.01]$ than the other groups (Table 1). They also showed a more rapid decline in MMSE and ADAS-cog during 24-month F/U (Table 1).

Discussion

As a result of the majority read by five independent reviewers, 8.4% of amyloid PET were deemed to be visually equivocal; this finding is in agreement with those of previous reports [5,6,8]. The equivocal group showed intermediate amyloid load between the negative and the positive group. The majority of them exceeded the positivity cut-off in terms of the SUVR. Furthermore, they were mostly below the positivity cut-off in CSF $A\beta_{1-42}$. According to the time course of biomarkers for AD [20,21], decreased CSF $A\beta_{1-42}$ preceded amyloid deposition in PET. Therefore, amyloid PET with equivocal visual findings might be a finding that was noted during the transition of a negative PET into a positive PET. This assumption is supported by the rapid amyloid accumulation during 24-month F/U, especially in patients with MCI.

In the model for biomarker changes, saturation of amyloid biomarkers is followed by neurodegeneration including cerebral glucose hypometabolism, brain volume, hippocampal atrophy, and cognition. Amyloid PET with visually positive findings in this study showed a similar pattern during 24-month F/U. In contrast, amyloid PET with visually negative findings remained unchanged in terms of both amyloid and neurodegeneration biomarkers.

In terms of equivocal PET, Hosokawa *et al.* [5] focused on the degree of cortical retention and defined it as suspected cortical accumulation, but not higher than that in the white matter by two reviewers. Conversely, Payoux *et al.* [6] focused on agreement and defined it as images with no consensus among three reviewers. In our current study, there were five reviewers and defined equivocal PET as images with narrow majority (no >4 reviewers with the same ratings) to prevent defining equivocal PET by a single reviewer's opinion. In clinical practice, we sometimes encounter amyloid PET that is difficult to designate as positive or negative. We tackled the problem of equivocal PET by reading it with multiple reviewers with majority reads and not by one reviewer. We believe that this solution is practical because it eliminates the need for any additional analytic software. We observed that interobserver variability on binary visual interpretation of fluorine-18-florbetapir PET was small, thus suggesting that having 100 practice cases after training with an electronic program may be enough for clinical purposes in most cases.

This study has several noteworthy limitations. First, combined CT scans were not available on the ADNI database. Anatomical imaging including MRI or computed tomography may help identify cortical gray matter, especially in cases of brain atrophy, and may reduce the number of equivocal cases. Second, the clinical F/U period was not long enough to assess the cognitive evolution of equivocal cases. Nevertheless, the clinical

diagnosis in the majority of patients remained unchanged, and only a few patients were converted to AD in each group. Third, only fluorine-18-florbetapir PET was assessed in our study. Although a recent systematic review and meta-analysis found no marked difference in the diagnostic accuracy of the three fluorine-18-labeled Aβ tracers [22], the different kinds of tracers may lead to distinct results, considering their different chemical structures and affinity for neuritic and diffuse plaque [21,23].

Conclusion

8.4% of patients from the ADNI cohort showed visually equivocal amyloid PET scans. The majority of these patients were quantitatively positive both in fluorine-18-florbetapir SUVR and in CSF $A\beta_{1-42}$, with relatively rapid amyloid accumulation.

Conflicts of interest

There are no conflicts of interest.

References

1 McKhann GM, Knopman DS, Chertkow H, Hyman BT, Jack CR, Kawas CH, et al. The diagnosis of dementia due to Alzheimer's disease: Recommendations from the National Institute on Aging-Alzheimer's Association workgroups on diagnostic guidelines for Alzheimer's disease. *Alzheimers Dement* 2011; **7**:263–269.

2 Ikonomovic MD, Klunk WE, Abrahamson EE, Mathis CA, Price JC, Tsopelas ND, et al. Post-mortem correlates of in vivo PiB-PET amyloid imaging in a typical case of Alzheimer's disease. *Brain* 2008; **131**:1630–1645.

3 Yang L, Rieves D, Ganley C. Brain amyloid imaging – FDA approval of florbetapir F18 injection. *N Engl J Med* 2012; **367**:885–887.

4 Hosokawa C, Ishii K, Kimura Y, Hyodo T, Hosono M, Sakaguchi K, et al. Performance of ¹¹C-Pittsburgh compound B PET binding potential images in the detection of amyloid deposits on equivocal static images. *J Nucl Med* 2015; **56**:1910–1915.

5 Hosokawa C, Ishii K, Hyodo T, Sakaguchi K, Usami K, Shimamoto K, et al. Investigation of ¹¹C-PiB equivocal PET findings. *Ann Nucl Med* 2015; **29**:164–169.

6 Payoux P, Delrieu J, Gallini A, Adel D, Salabert A, Hitzel A, et al. Cognitive and functional patterns of nondemented subjects with equivocal visual amyloid PET findings. *Eur J Nucl Med Mol Imaging* 2015; **42**:1459–1468.

7 Nayate A, Dubroff J, Schmitt J, Nasrallah I, Kishore R, Mankoff D, et al. Use of standardized uptake value ratios decreases interreader variability of [¹⁸F] florbetapir PET brain scan interpretation. *Am J Neuroradiol* 2015; **36**:1237–1244.

8 Yamane T, Ishii K, Sakata M, Ikari Y, Nishio T, Ishii K, et al. Inter-rater variability of visual interpretation and comparison with quantitative evaluation of ¹¹C-PiB PET amyloid images of the Japanese Alzheimer's Disease Neuroimaging Initiative (J-ADNI) multicenter study. *Eur J Nucl Med Mol Imaging* 2017; **44**:850–857.

9 Landau SM, Fero A, Baker SL, Koeppe R, Mintun M, Chen K, et al. Measurement of longitudinal β-amyloid change with (¹⁸)F-florbetapir PET and standardized uptake value ratios. *J Nucl Med* 2015; **56**:567–574.

10 Landau SM, Breault C, Joshi AD, Pontecorvo M, Mathis CA, Jagust WJ, et al. Amyloid-beta imaging with Pittsburgh compound B and florbetapir: comparing radiotracers and quantification methods. *J Nucl Med* 2013; **54**:70–77.

11 Landau SM, Marks SM, Mormino EC, Rabinovici GD, Oh H, O'Neil JP, et al. Association of lifetime cognitive engagement and low beta-amyloid deposition. *Arch Neurol* 2012; **69**:623–629.

12 Blautzik J, Brendel M, Sauerbeck J, Kotz S, Scheiwein F, Bartenstein P, et al. Reference region selection and the association between the rate of amyloid accumulation over time and the baseline amyloid burden. *Eur J Nucl Med Mol Imaging* 2017; **44**:1364–1374.

13 Joshi A, Koeppe RA, Fessler JA. Reducing between scanner differences in multi-center PET studies. *Neuroimage* 2009; **46**:154–159.

14 Johnson KA, Sperling RA, Gidicsin CM, Carmasin JS, Maye JE, Coleman RE, et al. Florbetapir (F18-AV-45) PET to assess amyloid burden in Alzheimer's disease dementia, mild cognitive impairment, and normal aging. *Alzheimers Dement* 2013; **9**:S72–S83.

15 Landau SM, Harvey D, Madison CM, Koeppe RA, Reiman EM, Foster NL, et al. Associations between cognitive, functional, and FDG-PET measures of decline in AD and MCI. *Neurobiol Aging* 2011; **32**:1207–1218.

16 Shaw LM, Vanderstichele H, Knapik-Czajka M, Clark CM, Aisen PS, Petersen RC, et al. Cerebrospinal fluid biomarker signature in Alzheimer's disease neuroimaging initiative subjects. *Ann Neurol* 2009; **65**:403–413.

17 Folstein MF, Folstein SE, McHugh PR. 'Mini-mental state'. A practical method for grading the cognitive state of patients for the clinician. *J Psychiatr Res* 1975; **12**:189–198.

18 Rey A. *L'examen clinique en psychologie [The clinical psychological examination]*. Paris: Presses Universitaires de France; 1964.

19 Rosen WG, Mohs RC, Davis KL. A new rating scale for Alzheimer's disease. *Am J Psychiatry* 1984; **141**:1356–1364.

20 Jack CR Jr, Knopman DS, Jagust WJ, Petersen RC, Weiner MW, Aisen PS, *et al*. Tracking pathophysiological processes in Alzheimer's disease: an updated hypothetical model of dynamic biomarkers. *Lancet Neurol* 2013; **12**:207–216.

21 Nordberg A, Rinne JO, Kadir A, Långström B. The use of PET in Alzheimer disease. *Nat Rev Neurol* 2010; **6**:78–87.

22 Morris E, Chalkidou A, Hammers A, Peacock J, Summers J, Keevil S. Diagnostic accuracy of ^{18}F amyloid PET tracers for the diagnosis of Alzheimer's disease: a systematic review and meta-analysis. *Eur J Nucl Med Mol Imaging* 2016; **43**:374–385.

23 Landau S, Thomas B, Thurfjell L, Schmidt M, Margolin R, Mintun M, *et al*. Amyloid PET imaging in Alzheimer's disease: a comparison of three radiotracers. *Eur J Nucl Med Mol Imaging* 2014; **41**:1398–1407.